Internet of Things Enabled Pomegranate Leaf Disease Detection and Classification using Cuckoo Search with Sparse Auto Encoder

P. Sindhu[1, a *] and G. Indirani[2,b]
[1]Assistant Professor, Department of Computer Science, , Mahatma Gandhi Govt. Arts College, Chalakkara, P.O New Mahe, Puducherry (UT), India
[2]Associate Professor, Department of Computer Science & Engineering, Govt. College of Engineering, Sengipatti, Thanjavur, Tamil Nadu, India
[1] psindumano1@gmail.com [2]induk0992@gmail.com

.

Article Info
Page Number: 904 – 917
Publication Issue:
Vol. 71 No. 3 (2022)

Abstract
Recent technological advancements in the field of Internet of Things (IoT) and computer vision (CV) enable proper identification of plant diseases, which is a major challenge in agricultural productivity. Since plant leaf diseases mainly affect crop productivity and quality, earlier recognition of diseases becomes essential. The latest developments of deep learning (DL) models enable us to effectually categorize the existence of pomegranate leaf diseases. Therefore, this article develops an IoT Enabled Pomegranate Leaf Disease Detection and Classification using Cuckoo Search with Sparse Autoencoder (PLDDC-CSSAE) model. The presented PLDDC-CSSAE model determines appropriate class labels of the pomegranate leaf diseases accurately and rapidly. The PLDDC-CSSAE model initially employs Gaussian filtering-based noise removal with Shannon entropy based image segmentation. Next, NasNet model is exploited to produce high level deep features and finally, cuckoo search (CS) algorithm with SAE model is utilized for classification. The CS algorithm aids in the appropriate parameter choice of the SAE model and consequently resulting in enhanced performance. The PLDDC-CSSAE model shows better result over other methods by using benchmark dataset..

Article History
Article Received: *12 January 2022*
Revised: *25 February 2022*
Accepted: *20 April 2022*
Publication: *09 June 2022*

Keywords:- Pomegranate, Plant leaf diseases, Sparseautoencoder, Cuckoo search, Image segmentation.

Introduction

All manuscripts must be in English, also the table and figure texts, otherwise, we cannot publish IoT has caught the client's advantage as they help in observing and data storage in large-scale environments. Fostering the advances for expanding agriculture creation can help the economy of numerous nations [1, 2]. The agriculture misfortune can be principally because of the climatic change, nuisances, and diseases happening in the different seasons. Fostering the easy to understand climate change utilizing the IoT gadgets can help in further developing the agriculture creation. The IoT climate effectively associates the ranchers with the wide scope of harvests and makes cultivating simpler [3]. Accuracy Agriculture assists ranchers to outfit oneself with adequate and monetary data and control innovation because of improvement and openness in different fields. The targets are the ascent in benefits, the systematization of horticultural sources of info, and the decrease of ecological harm [4, 5]. Pomegranate (Punicagranatum) is a deciduous tree filled in dry and semiarid areas [6]. It fills well in regions with temperatures going from 25-35 degrees and yearly precipitation of 500-800 mm. As of late, diseases have brought about colossal misfortunes in pomegranate delivery. These diseases are typically brought about by miniature creatures like organisms, microorganisms, and infections [7]. Just agriculture masters or extremely experienced ranchers can know the sort of diseases and irritations on plants.

Farmers need to welcome the agriculture master to their homesteads or ranchers need to take the example from the ranch to agriculture research focus. Diseases are liable for financial, social, and environmental misfortunes. These diseases should be controlled at introductory phase of contamination. A portion of the diseases is exceptionally difficult to control in next phase of contamination [8]. Plant disease location framework initially catching picture by picture sensor gadgets, preprocessing procedure on diseased plant leaf or organic product picture, Split the picture into various fragments utilizing division method, highlight determination, and extraction, natural product or leaf disease ID utilizing order [9]. The plant leaf, organic product, or stem are principal visual pieces of plants showing the disease indications. Consequently, utilization of delicate registering method to find and group diseases in horticultural applications is valuable [10]. Pomegranate is one of the business and dry season lenient yields. Pomegranate cultivators are fundamental piece of the agriculture area in India where they present critical offers in agriculture economy.

Madhavan et al. [11] centre on planning a structure that can perceive and group diseases on pomegranate plants precisely. The system uses picture handling strategies, for example, picture securing, picture resizing, picture upgrade, picture division, ROI extraction (area of interest), and element extraction. A picture dataset connected with pomegranate leaf disease is used to execute the structure, separated as to preparation set and a test set. In the execution interaction, strategies, for example, picture upgrade and picture division are principally utilized for distinguishing ROI and elements. A picture order will then, at that point, be carried out by joining support vector machine. Mostafa et al. [12] utilize a deep convolutional brain organization (DCNN)-based information improvement to recognize different guava plant species. Nine points from 360∘were applied to expand the number of changed plant pictures. This increased information was then taken care of as a contribution to cutting-edge arrangement organizations.

Sánchez et al. [13] proposed another strategy to distinguish and characterize Botrytis disease of the pomegranate through consolidating AI procedures. The strategy utilizes various procedures, for example, Gaussian channel, morphological activities, among others, to separate the picture highlights. Doppala et al. [14] proposed a CNN model for the precise disease expectation. Detection of the plant disease incorporates strategies like picture isolation, preprocessing, fragmentation of the picture, location, and acknowledgment of qualities. This paper principally inspects the limiting division and recovery elements of predominantly on two various plant diseases (pomegranate and potato).

The proposed model develops an IoT Enabled Pomegranate Leaf Disease Detection and Classification using Cuckoo Search with Sparse Autoencoder (PLDDC-CSSAE) model. Initially it employs Gaussian filtering based noise removal with Shannon entropy based image segmentation. Then ,NasNet model is exploited to produce high level deep features and in the final step ,cuckoo search (CS) algorithm with SAE model is utilized for classification. For appropriate parameter selection of SAE model and enhanced performance CS algorithm is used here. The experimental validation of the PLDDC-CSSAE model shows better result over the other methods on real-world dataset.

The Proposed Model

In this study, a novel PLDDC-CSSAE model has been developed to determine appropriate class labels of the pomegranate leaf diseases accurately and rapidly in the IoT environment. Primarily, data augmentation process is carried out using three ways such as rotate, horizontal flip, and vertical flip. The PLDDC-CSSAE model initially employs Gaussian filtering-based noise removal with Shannon entropy-based image segmentation. Next, NasNet model is exploited to produce high level deep features and finally, CS algorithm with SAE model is utilized for classification. Fig. 1 illustrates the block diagram of PLDDC-CSSAE technique.

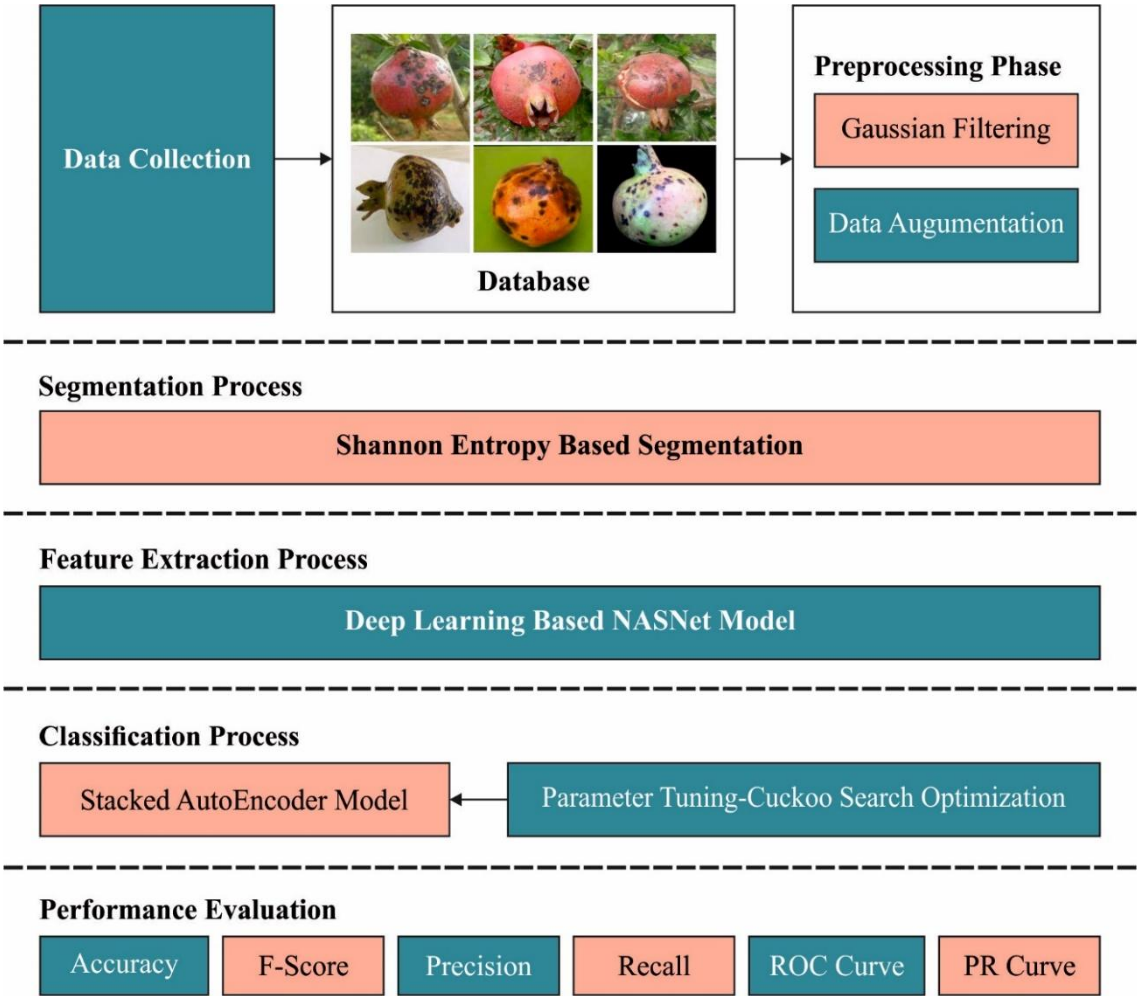

Fig. 1: Block diagram of PLDDC-CSSAE technique

Level I: Image Segmentation

Primarily, the pomegranate leaf images are pre-processed and then segmented using Shannon's entropy. Shannon's entropy (SE) technique is a vital model in the domain of "information theory and coding". This model was employed for probabilistically defining the amount of data transferred with around data. Assume that an image is $(k+1)$ homogeneous region and k threshold gray level at $t_1, t_2, t_3, \dots, t_k$.

$$h(i) = \frac{f_i}{N} \; i = 0,1,2,,255.$$

whereasf_i implies the frequency of i^{th} gray levels, N refers the whole count of gray levels present in the images, and $h(i)$ demonstrates the normalized frequency. The SE function is demonstrated as:

$$H = -\sum_{i=0}^{t_1} P_{1i} \ln(P_{1i}) - \sum_{i=t_1+1}^{t_2} P_{2i} \ln(P_{2i}) - \cdots - \sum_{i=t_k}^{255} P_{ki} \ln(P_{ki}) \qquad (1)$$

whereas,

$$P_{1i} = \frac{h(i)}{\sum_{i=0}^{t_1} h(i)} \; for \; 0 \le i \le t_1,$$

$$P_{2i} = \frac{h(i)}{\sum_{i=t_1+1}^{t_2} h(i)} \; for \; t_1 + 1 \le i \le t_2,$$

$$P_{ki} = \frac{h(i)}{\sum_{i=t_k+1}^{255} h(i)} \; for \; t_k + 1 \le i \le 255.$$

Level II: Feature Extraction

Once the images are segmented, the high level deep features are produced by the NASNet model [15]. The NASNetMobile architecture is a newly established DL technique using 53,26,716parameters. It shows higher consistency. The central module of the NASNet architecture is the block and a group of blocks is collectively combined to create a cell. The search space included in the NASNet is the factoring of the network to cells and separated into sub-blocks. The type and number of blocks or cells are not predetermined. But they need to be augmented for the select data set. The feasible function of the blocks encompasses max pooling, convolution, separable convolution, identify map, average pooling, and so on. All the blocks have the capacity to map two inputs into output feature mapping. It executes element wise adding. Once the cell obtains a block through feature mapping size of H × W and stride of 1, result would be the equal size of the featured mapping. When the stride is 2, the size is reduced to 2. The cells are incorporated into optimized technique. The system progression is concentrated with 3 features: the amount of cells that stacked (N), the quantity of filters from the main layer (F), and the cell infrastructure. Primarily N and F are set in the search. Next, N and F from the primary layer are altered to control the width and depth of systems. When the search was completed, method is formed by numerous sizes to fit the dataset. Then, the cell is associated with an optimized technique to design for the NASNet structure. Each cell is related with 2 input layers called as hidden layer. To offer high performance NASNetLarge is attained N as 6. However, the fundamental block concern to NASNetMobileis run through controlled source. An approach called scheduled drop path was suggested in NASNet, in which each path from the cell was dropped by linearly improving possibility as trained of network progression.

Level III: Image Classification

The generated high level deep features are passed into the SAE model for plant leaf disease classification [16]. SAE generally tries to learn an approximation function in any criteria of constraints, like limiting the number of hidden units and assigning sparsity constraints on the hidden unit, therefore that the number of resultant units y has infinitely close (equivalent) to the amount of input units x.

$$Z_j^{(l)} = \sum_{j=1}^{n} W_{ij}^{(l-1)} y_j^{(l-1)} + b_i^{(l)} = h_{W,b}(y_j^{l-1}),$$

$$y_j^{(l)} = f\left(z_j^{(l)}\right). \tag{2}$$

The minimizing cost function is defined as:

$$J(W,b) = \left[\frac{1}{m}\sum_{i=1}^{m}\left(\frac{1}{2}\left\|a^{(3)(i)} - x^{(i)}\right\|^2\right)\right] + \frac{\lambda}{2}\sum_{l=1}^{n_l-2}\sum_{i=1}^{s_l}\sum_{j=1}^{s_{l+1}}\left(W_{ji}^{(l)}\right)^2 \tag{3}$$

In (2), an initial term reflects the distance amongst the input and output, and the second term is a regularized which incline cut-down the weight and is utilized for preventing over-fit; the parameter λ controls the weighted amongst the 2 terms. For ensuring the feature bear a wanted sparsity from the hidden layer, a sparsity constraint, utilized to control the learning procedure was established as to the cost functions. This sparsity constraint creates the hidden unit to be inactive nearly. The equivalent average activation of j^{th} hidden unit is provided as:

$$\hat{\rho}_{\mathrm{j}} = \frac{1}{m}\sum_{i=1}^{m}\left(a_j^{(2)} x^{(i)}\right). \tag{4}$$

For making $\hat{\rho}_j$ developed a very small value ρ, the sparsity penalty term is provided dependent upon the Kullback - Leibler (KL) divergence method:

$$KL(\rho\|\hat{\rho}) = \rho \log \frac{\rho}{\hat{\rho}_j} + (1-\rho)\log\frac{1-\rho}{1-\hat{\rho}_j}. \tag{5}$$

Therefore, this sparsity penalty term has assumed that the subsequent cost function:

$$J_{sparse}\,(W,b) = J(W,b) + \beta \sum_{j} KL(\rho \| \hat{\rho}), \tag{6}$$

whereasβ signifies the weighted sparsity penalty term.

Level IV: Parameter Optimization

At this stage, the CS algorithm aids in the appropriate parameter choice of the SAE model and consequently resulting in enhanced performance [17, 18]. CS approach was inspired by the social performance of Cuckoos. In the mathematical model, the CS technique is stated in 3 important levels. The next position is every Cuckoo place only a single egg at timestamp to arbitrarily selected host nest and lastly, the maximal quality eggs in the optimal nest were surplus to next generation. Consider that $X_i(t)$ refers the current searching space of Cuckoo $i, where\ i = 1, 2, \cdots, N$ at a time t, signified as $X_i = (x_i^1, x_i^2, \cdots\cdots, x_i^n)$ from the n dimensional quandary. Next, a primary searching space $X_i(t+1)$ to later generation at time $t+1$is mathematically estimated as:

$$X_i(t+1) = X_i(t) + \alpha Levy(\lambda) \tag{7}$$

whereas$\alpha > 0$ stands for the step-size which is same as the scale of quandaries of the curiosity, in higher cases α is usually obtained as 1. It offers an arbitrary walk and their arbitrary stages are drawn in Levy distribution for immensely colossal stages that are signified as:

$$Levy\ (\lambda)u = t^{-\lambda}, where\ 1 < \lambda < 3 \tag{8}$$

The 2 very famous approaches are Mantegna's method and McCulloch's method. The Levy step size is gained in the Mantegna approach as initialization

$$Levy = \frac{\upsilon}{|\nu|^{1/(\lambda-1)}} \tag{9}$$

The condition as forsake probability, the whole size of populations, and higher count of reproducing of cuckoo in the lifespan was set to utilizer; yet, a primary term at the initial is attained.

Considered that t represents the present generation, t_{max} denotes the maximum number of iterations.

$$x_1^n(t=1) = randn \times (Upper^n - Lower^n) \tag{10}$$

whereas$Lower^n$ and $Upper^n$ defines the lowermost and uppermost outer restricts of searching space of n^{th} attribute correspondingly. This keeps the mastery capable time optimizing manner stay from the individual perimeter. Fig. 2 demonstrates the flowchart of CS technique.

In Eq. (9), υ and ν represent the taken in normal distribution. In other words $\upsilon \sim N\ (0, \delta^2)$ and $\nu \sim N\ (0, 1)$ with

$$\delta = \left(\frac{\Gamma(1+\beta)\sin\left(\frac{\pi\pi}{2}\right)}{\Gamma\left(\frac{1+\beta}{2}\right)\beta \times 2^{\left(\frac{\beta-1}{2}\right)}} \right)^{\frac{1}{\beta}} \tag{11}$$

In which Γ stands for the gamma function and it could be represented as:

$$\Gamma(p) = \int_0 e^{-t}\, t^{p-1} dt \& \beta \in [0,2]\ is\ a\ scale\ factor. \tag{12}$$

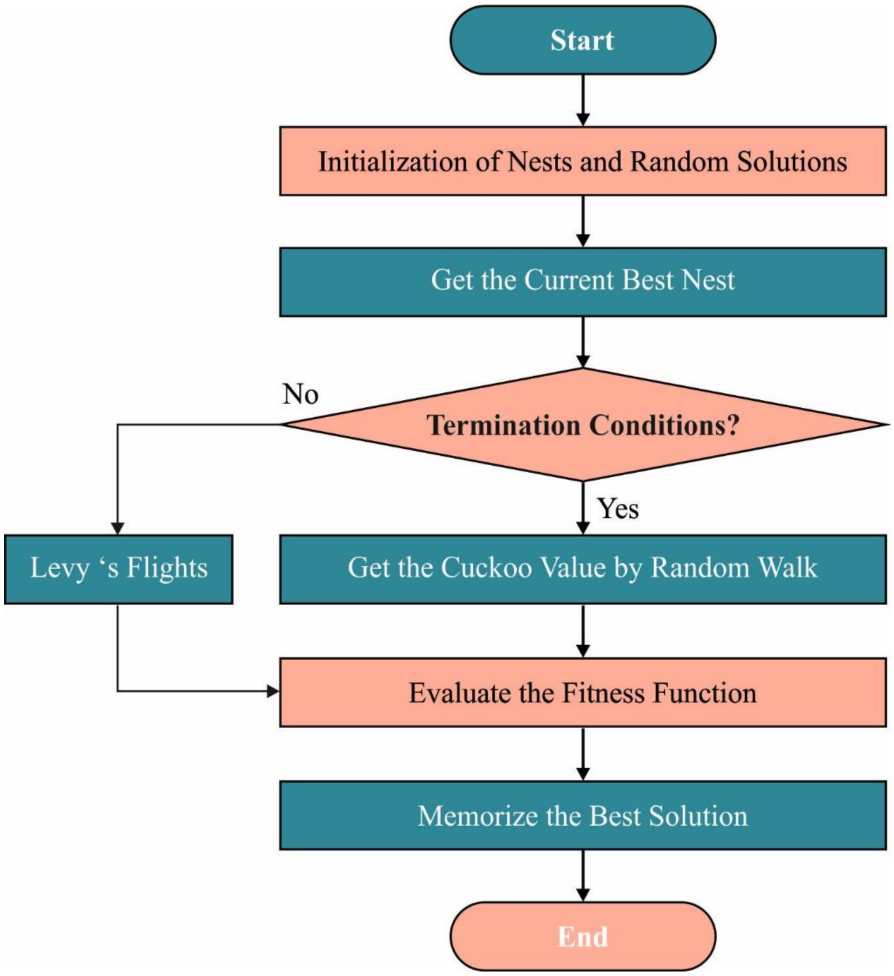

Figure. 2. Flowchart of CS technique

Results and Discussion

In this section, a brief examination of the PLDDC-CSSAE model on test pomegranate leaf disease images takes place. Originally, the dataset a set of 50 images existed under three classes Anthracnose, Bacterial Blight, and Cercospora. After data augmentation, the number of images under Anthracnose, Bacterial Blight, and Cercospora class becomes 200. Fig. 3 depicts a few sample images.

Figure 3: Sample images

Fig. 4 reports a set of confusion matrices offered by the PLDDC-CSSAE model on distinct sizes of TR/TS datasets. On TR/TS data of 90:10, the PLDDC-CSSAE model has identified 22, 26, and 11 samples under Anthracnose, Bacterial Blight, and Cercospora classes respectively. Also, on TR/TS data of 80:20, the PLDDC-CSSAE approach has identified 38, 38, and 41 samples under Anthracnose, Bacterial Blight, and Cercospora classes correspondingly. Meanwhile, on TR/TS data of 70:30, the PLDDC-CSSAE model has identified 51, 61, and 66 samples under Anthracnose, Bacterial Blight, and Cercospora classes respectively. Followed by, on TR/TS data of 60:40, the PLDDC-CSSAE method has identified 84, 78, and 75 samples under Anthracnose, Bacterial Blight, and Cercospora classes correspondingly.

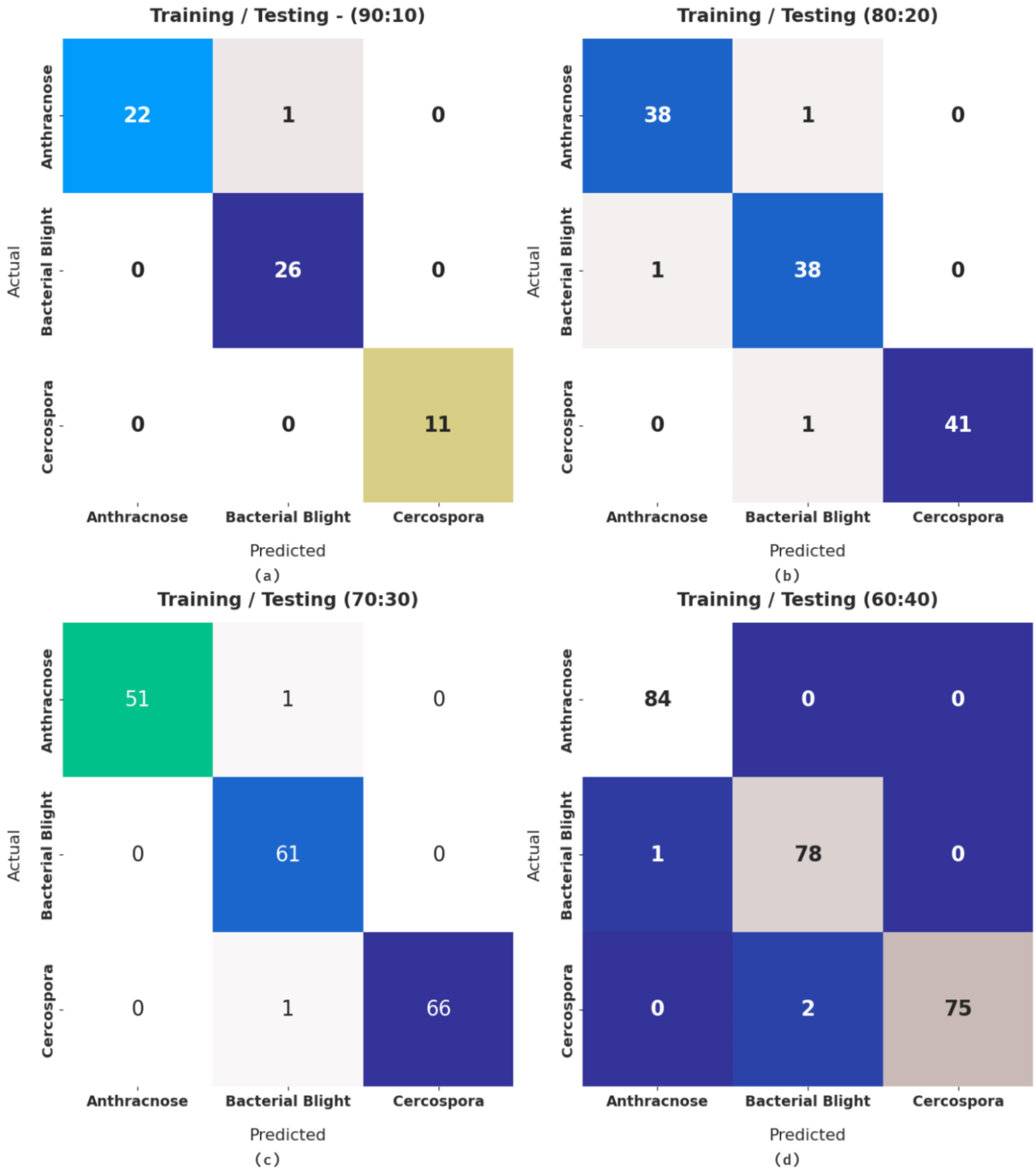

Fig. 4: Confusion matrix of PLDDC-CSSAE technique on distinct sizes of TR/TS datasets

Table 1 and Fig. 5 reports extensive classification outcomes of the PLDDC-CSSAE model on distinct sizes of TR/TS data. The experimental results indicated that the PLDDC-CSSAE model has reached maximum values under all sizes of TR/TS data. For instance, with TR/TS data of 90:10, the PLDDC-CSSAE model has offered $accu_y$ of 98.89%, $prec_n$ of 98.77%, $reca_l$ of 98.55%, and F_{score} of 98.63%. In addition, with TR/TS data of 80:20, the PLDDC-CSSAE system has obtainable $accu_y$ of 98.33%, $prec_n$ of 97.48%, $reca_l$ of 97.50%, and F_{score} of 97.48%. Also, with TR/TS data of 70:30, the PLDDC-CSSAE method has offered $accu_y$ of 99.26%, $prec_n$ of 98.94%, $reca_l$ of 98.86%, and F_{score} of 98.89%. Lastly, with TR/TS data of 60:40, the PLDDC-CSSAE approach has offered $accu_y$ of 99.17%, $prec_n$ of 98.77%, $reca_l$ of 98.71%, and F_{score} of 98.74%.

Table 1: Result analysis of PLDDC-CSSAE approach with distinct measures

Class Labels	Accuracy	Precision	Recall	F-Score
Training / Testing (90:10)				
Anthracnose	98.33	100.00	95.65	97.78
Bacterial Blight	98.33	96.30	100.00	98.11
Cercospora	100.00	100.00	100.00	100.00
Average	**98.89**	**98.77**	**98.55**	**98.63**
Training / Testing (80:20)				
Anthracnose	98.33	97.44	97.44	97.44
Bacterial Blight	97.50	95.00	97.44	96.20
Cercospora	99.17	100.00	97.62	98.80
Average	**98.33**	**97.48**	**97.50**	**97.48**
Training / Testing (70:30)				
Anthracnose	99.44	100.00	98.08	99.03
Bacterial Blight	98.89	96.83	100.00	98.39
Cercospora	99.44	100.00	98.51	99.25
Average	**99.26**	**98.94**	**98.86**	**98.89**
Training / Testing (60:40)				
Anthracnose	99.58	98.82	100.00	99.41
Bacterial Blight	98.75	97.50	98.73	98.11
Cercospora	99.17	100.00	97.40	98.68
Average	**99.17**	**98.77**	**98.71**	**98.74**

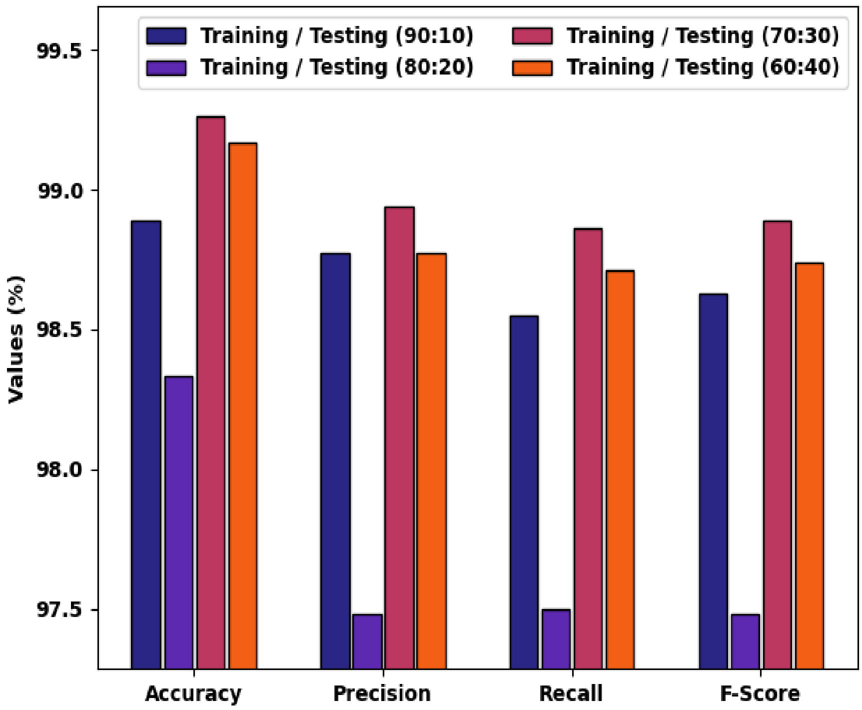

Figure 5: Result analysis of PLDDC-CSSAE algorithm with distinct measures

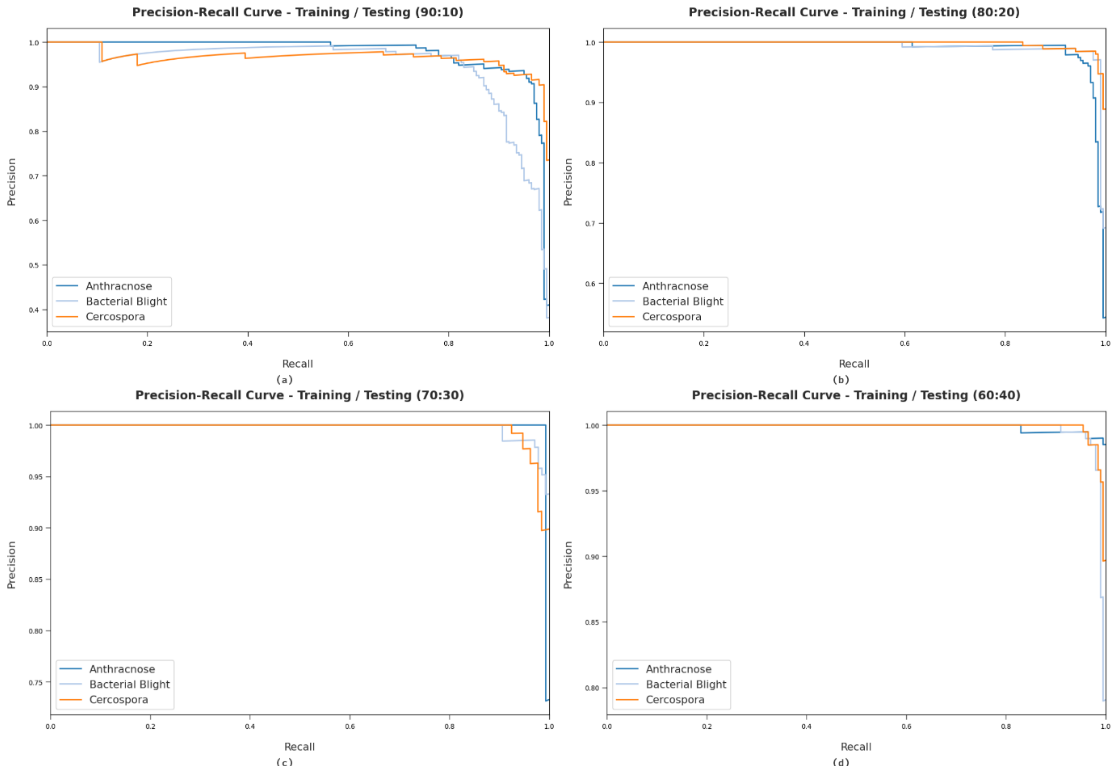

Fig. 6: Precision-recall analysis of PLDDC-CSSAE technique with distinct sizes of TR/TS datasets

A brief precision-recall examination of the PLDDC-CSSAE model on different TR/TS datasets is portrayed in Fig. 6. By observing the figure, it is noticed that the PLDDC-CSSAE model has accomplished maximum precision-recall performance under all datasets.

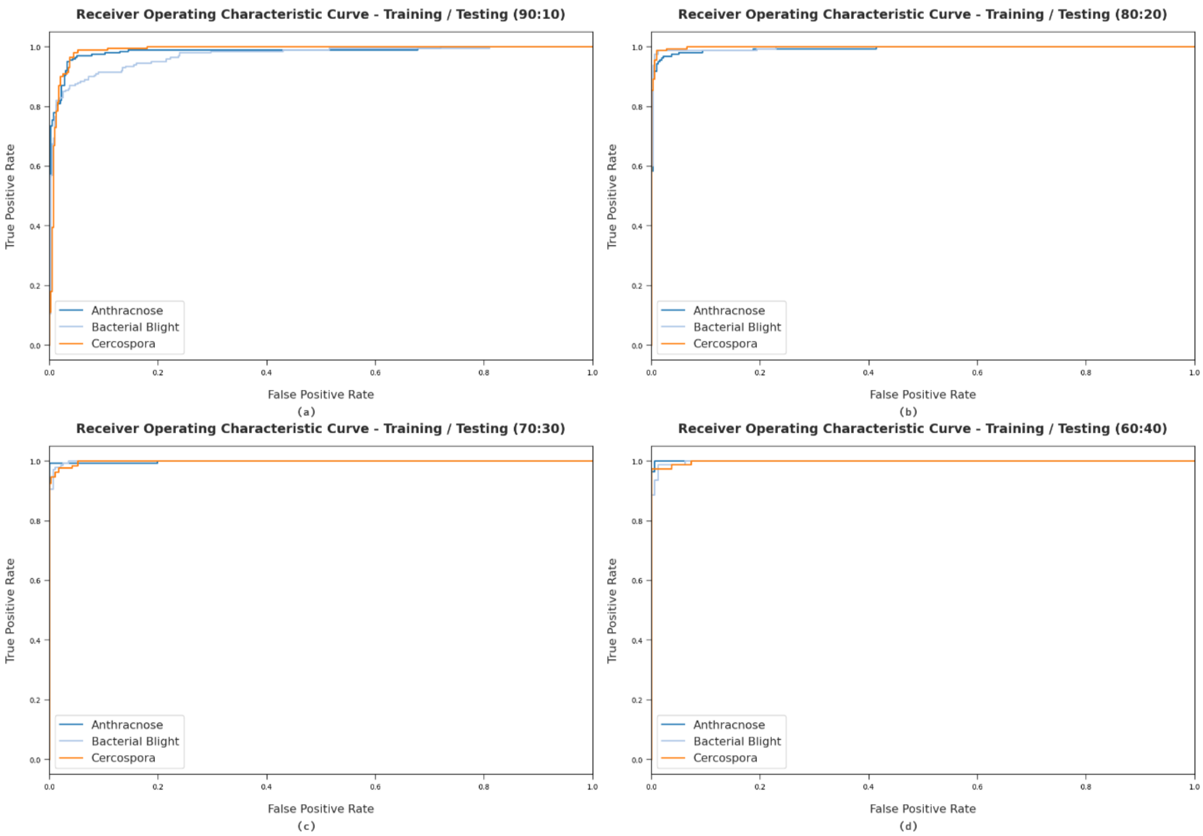

Fig.ure 7: ROC analysis of PLDDC-CSSAE technique with distinct sizes of TR/TS datasets

A detailed ROC investigation of the PLDDC-CSSAE model on the distinct TR/TS datasets is portrayed in Fig. 7. The results indicated that the PLDDC-CSSAE model has exhibited its ability in categorizing three different classes such as Anthracnose, Bacterial Blight, and Cercospora on the test datasets.

Finally, a comprehensive comparative study of the PLDDC-CSSAE model with other models on pomegranate leaf disease classification is shown in Table 2. The experimental values indicated that the PLDDC-CSSAE model has accomplished effectual outcomes over the existing methods.

Fig. 8 highlights a comparative examination of the PLDDC-CSSAE model with other models in terms of $accu_y$. The experimental results implied that the SVM model has resulted to lower $accu_y$ of 76.18%. Next to that, the backpropagation model has reached slightly improved performance with $accu_y$ of 89.56%. Along with that, the ANN and Adaboost models have obtained certainly improved $accu_y$ of 92.49% and 92.44% respectively. Though the CNN-LSTM model has accomplished reasonable $accu_y$ of 98.57%, the presented PLDDC-CSSAE technique has demonstrated the other algorithms with maximum $accu_y$ of 99.26%.

Table 2: Comparative analysis of PLDDC-CSSAE method with existing algorithms

Methods	**Accuracy**	**Precision**	**Recall**
CNN-LSTM Model	98.57	97.83	96.74
Ada Boost Model	92.44	93.39	93.88
Back Propogation Model	89.56	90.64	90.20
SVM Model	76.18	75.05	74.13
ANN Model	92.49	92.37	92.94
PLDDC-CSSAE	99.26	98.94	98.86

Fig. 9 demonstrates a comparative examination of the PLDDC-CSSAE approach with other models in terms of $prec_n$. The experimental results implied that the SVM model has resulted to lower $prec_n$ of 75.05%. Next to that, the back propagation system has reached slightly improved performance with $prec_n$ of 90.64%. Along with that, the ANN and Adaboost methods have obtained certainly enhanced $prec_n$ of 92.37% and 93.39% respectively. Eventually, the CNN-LSTM algorithm has accomplished reasonably $accu_y$ of 97.83%, the presented PLDDC-CSSAE methodology has outperformed the other methods with maximum $prec_n$ of 98.94%.

Fig. 10 examines a comparative examination of the PLDDC-CSSAE technique with other models with respect to $reca_l$. The experimental results implied that the SVM model has resulted to lower $reca_l$ of 74.13%. Next to that, the back propagation approach has reached somewhat improved performance with $reca_l$ of 90.20%. Along with that, the ANN and Adaboost models have obtained certainly improved $reca_l$ of 92.94% and 93.88% correspondingly. Finally, the CNN-LSTM technique has accomplished reasonably $reca_l$ of 96.74%, the presented PLDDC-CSSAE algorithm has outperformed the other methods with maximum $reca_l$ of 98.86%.

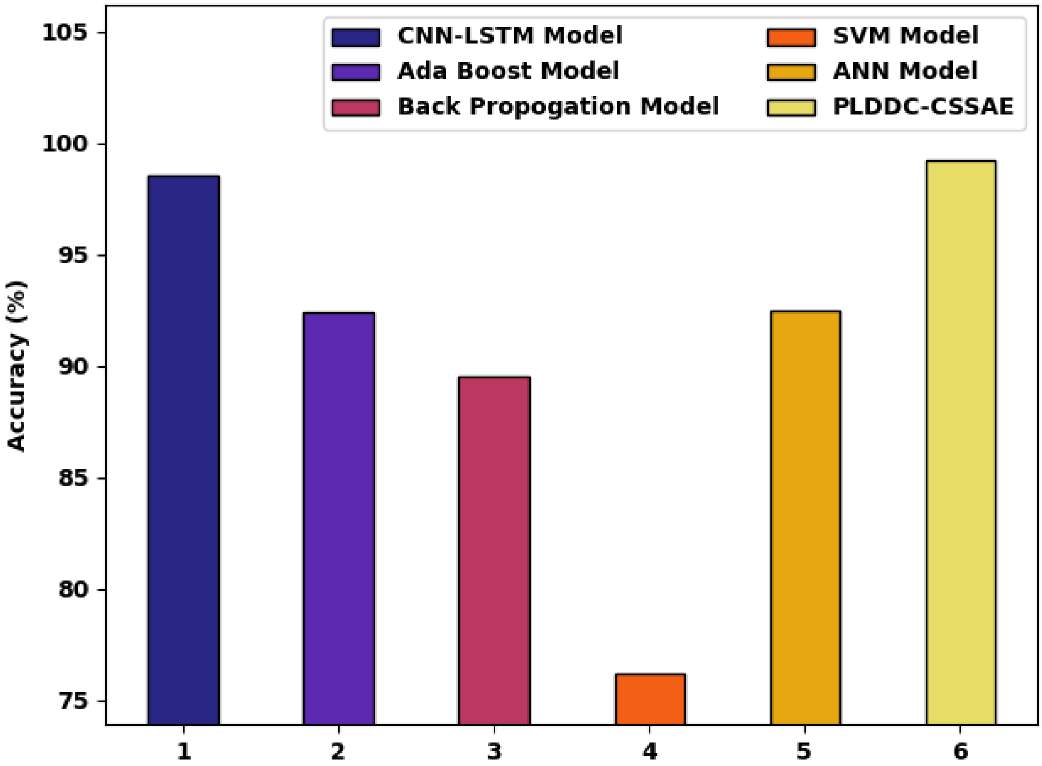

Figure 8: Acc_y **analysis of PLDDC-CSSAE technique with existing methods**

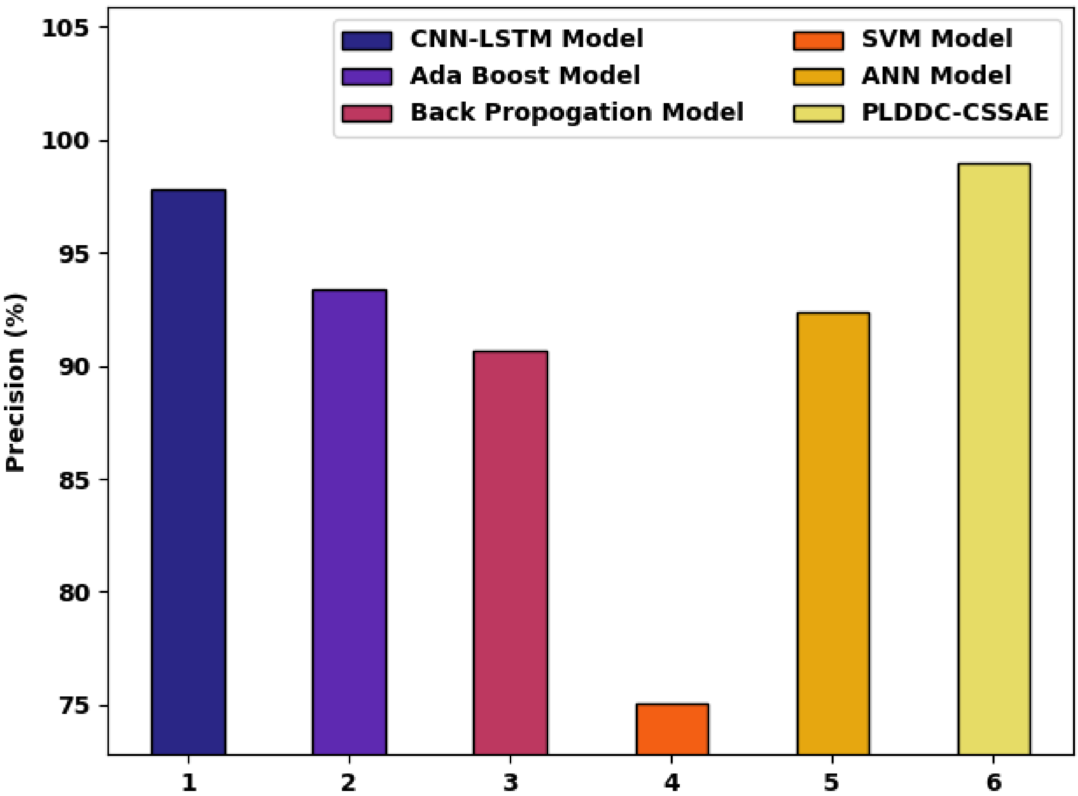

Fig. 9: $Prec_n$ **analysis of PLDDC-CSSAE technique with existing methods**

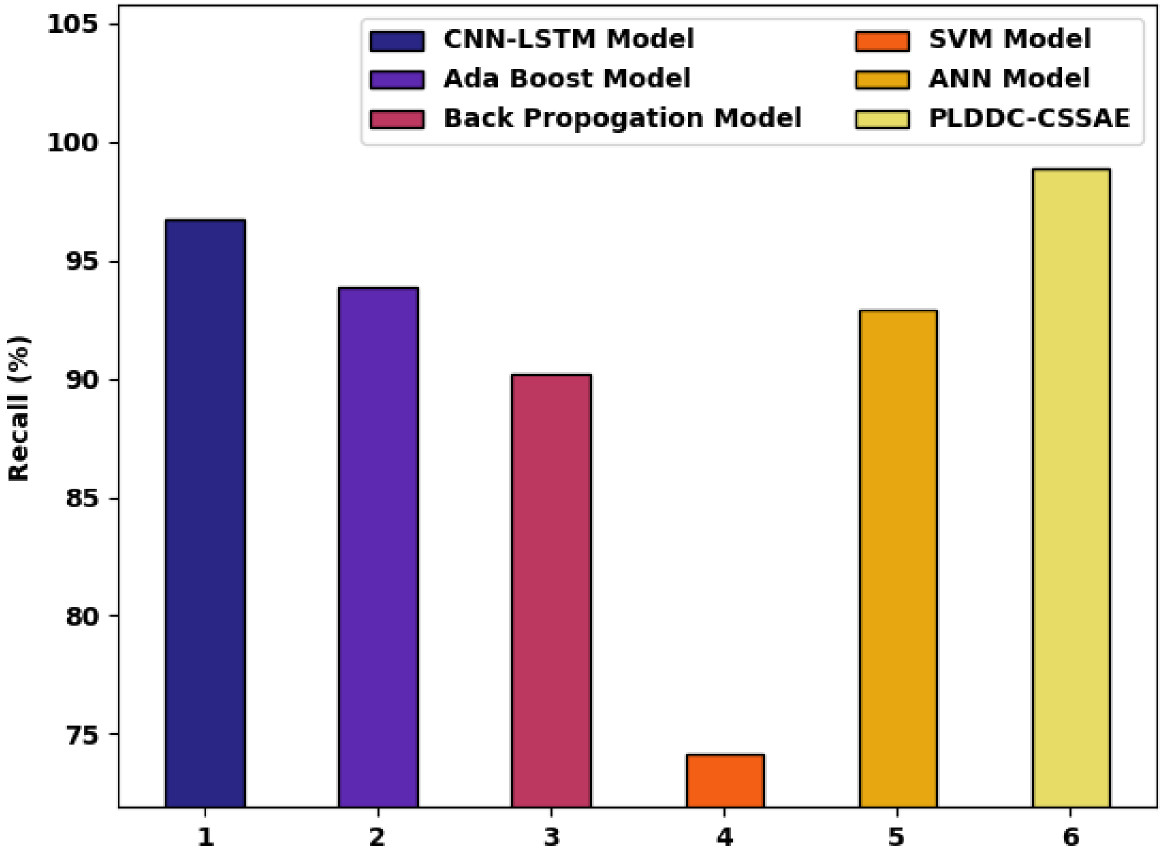

Fig. 10: $\boldsymbol{Reca_l}$ **analysis of PLDDC-CSSAE technique with existing methods**

After examining the results and discussion, it is clearly noticed that the PLDDC-CSSAE model has the ability to attain effectual outcomes on pomegranate leaf disease detection and classification.

Conclusion

In this study, a novel PLDDC-CSSAE model has been developed to determine appropriate class labels of the pomegranate leaf diseases accurately and rapidly in the IoT environment. The PLDDC-CSSAE model begins by removing noise using Gaussian filtering followed by picture segmentation using Shannon entropy. Following that, a NasNet model is used to generate high-level deep features, and ultimately, a CS algorithm combined with an SAE model is used for classification. The CS algorithm aids in the proper parameter selection of the SAE model, resulting in improved performance. Experiments validating the PLDDC-CSSAE model demonstrated that it outperformed other techniques on the benchmark dataset. Thus, the PLDDC-CSSAE model has appeared as an effectual tool for pomegranate disease detection.

Reference

[1] Singh, J., 2021. Automated Disease Detection and Classification of Plants Using Image Processing Approaches: A Review. In *Proceedings of Second International Conference on Computing, Communications, and Cyber-Security* (pp. 641-651). Springer, Singapore.

[2] Singh, V., Sharma, N. and Singh, S., 2020. A review of imaging techniques for plant disease detection. *Artificial Intelligence in Agriculture*, *4*, pp.229-242.

[3] Nirmalakumari, K., Rajaguru, H. and Rajkumar, P., 2019, September. Plant Leaf Disease Detection Using Modified Segmentation Process and Classification. In *International Conference On Computational Vision and Bio Inspired Computing* (pp. 442-452). Springer, Cham.

[4] Prabha, D.R., Swaminathan, R., Chaitanya, K. and Sultana, W.R., 2019. Arduino Based Smart Irrigation System and Plant Leaf Disease Detection Using MATLAB. *International Journal of Mechanical Engineering and Technology*, *10*(12).

[5] Singh, V., 2019. Sunflower leaf diseases detection using image segmentation based on particle swarm optimization. *Artificial Intelligence in Agriculture*, *3*, pp.62-68.

[6] Vasumathi, M.T. and Kamarasan, M., 2021. An Effective Pomegranate Fruit Classification Based On CNN-LSTM Deep Learning Models. *Indian Journal of Science and Technology*, *14*(16), pp.1310-1319.

[7] Kadoli, V., Gull, K.C. and Gull, S.C., 2021. Dissimilar Disease Detection Using Machine Learning Techniques for Variety of Leaves. In *Sustainable Communication Networks and Application* (pp. 57-71). Springer, Singapore.

[8] Karthickmanoj, R., Padmapriya, J. and Sasilatha, T., 2021. A novel pixel replacement-based segmentation and double feature extraction techniques for efficient classification of plant leaf diseases. *Materials Today: Proceedings*, *47*, pp.2048-2052.

[9] Deepalakshmi, P., Lavanya, K. and Srinivasu, P.N., 2021. Plant leaf disease detection using CNN algorithm. *International Journal of Information System Modeling and Design (IJISMD)*, *12*(1), pp.1-21.

[10] Kavitha Lakshmi, R. and Savarimuthu, N., 2021. DPD-DS for plant disease detection based on instance segmentation. *Journal of Ambient Intelligence and Humanized Computing*, pp.1-11.

[11] Madhavan, M.V., Thanh, D.N.H., Khamparia, A., Pande S, M.R. and Gupta, D., 2021. Recognition and classification of pomegranate leaves diseases by image processing and machine learning techniques. Computers, Materials & Continua, 66(3), pp.2939-2955.

[12] Mostafa, A.M., Kumar, S.A., Meraj, T., Rauf, H.T., Alnuaim, A.A. and Alkhayyal, M.A., 2021. Guava Disease Detection Using Deep Convolutional Neural Networks: A Case Study of Guava Plants. Applied Sciences, 12(1), p.239.

[13] Sánchez, M.G., Miramontes-Varo, V., Chocoteco, J.A. and Vidal, V., 2020, July. Identification and classification of botrytis disease in pomegranate with machine learning. In Science and Information Conference (pp. 582-598). Springer, Cham.

[14] Doppala, B.P., Bandi, V., Rao, N.T. and Bhattacharyya, D., 2022. A Hybrid Intelligent Approach for Early Identification of Different Diseases in Plants. In Machine Intelligence and Soft Computing (pp. 25-32). Springer, Singapore.

[15] Bharati, S., Podder, P., Mondal, M. and Gandhi, N., 2020, December. Optimized NASNet for diagnosis of COVID-19 from lung CT images. In *International Conference on Intelligent Systems Design and Applications* (pp. 647-656). Springer, Cham.

[16] Xu, J., Xiang, L., Liu, Q., Gilmore, H., Wu, J., Tang, J. and Madabhushi, A., 2015. Stacked sparse autoencoder (SSAE) for nuclei detection onbreast cancer histopathology images. *IEEE transactions on medical imaging*, *35*(1), pp.119-130.

[17] Mareli, M. and Twala, B., 2018. An adaptive Cuckoo search algorithm for optimisation. *Applied computing and informatics*, *14*(2), pp.107-115.

[18] Valian, E., Mohanna, S. and Tavakoli, S., 2011. Improved cuckoo search algorithm for global optimization. *International Journal of Communications and Information Technology*, *1*(1), pp.31-44.